ChemComm

COMMUNICATION

View Article Online
View Journal | View Issue

Cite this: *Chem. Commun.*, 2019, **55**, 2533

Received 4th January 2019,
Accepted 1st February 2019

DOI: 10.1039/c9cc00066f

rsc.li/chemcomm

A ratiometric fluorescent probe for detecting hypochlorite in the endoplasmic reticulum†

Ji-Ting Hou,‡[ab] Hyeong Seok Kim,‡[c] Chong Duan,‡[d] Myung Sun Ji,[c] Shan Wang,*[ab] Lintao Zeng,*[d] Wen Xiu Ren*[ef] and Jong Seung Kim*[c]

A colorimetric and fluorescent probe ER-ClO was presented in this work to detect cellular hypochlorite with high selectivity and sensitivity. With an organelle targeting unit, ER-ClO was successfully applied in the bio-imaging of exogenous and endogenous hypochlorite in the endoplasmic reticulum in a ratiometric manner.

The endoplasmic reticulum (ER), a membrane-rich structure found in all eukaryotes, is the largest cellular organelle. It is responsible for the synthesis, folding, modification, and delivery of proteins,[1] and most of the intracellular Ca^{2+} is stored in the ER.[2] The dysfunction of the ER, usually called ER stress, induces an unfolded protein response (UPR) in the ER,[3] and mediates complicated signaling pathways. Increased ER stress can even be associated with heart disease, stroke, neurodegenerative disorders, and cancer.[4] Hence, the ER has recently been recognized as an important target for cancer therapy.[5] Among the factors initiating ER stress, reactive oxygen species (ROS), including $^{\bullet}OH$, $O_2^{\bullet-}$, $ONOO^-$, H_2O_2, ClO^-, and $^1O_2$, have been identified to play vital roles in the UPR owing to their strong oxidability.[6] However, the exact association between ROS and ER activity has not been sufficiently revealed yet because of the lack of reliable techniques. Therefore, it is of extraordinary value to exploit novel tools to monitor ROS variation in the ER for understanding the redox circumstance in the ER, thus assessing the ER status.

Nowadays, fluorometric analysis has attracted worldwide attention in bioimaging for its high sensitivity, excellent temporal and spatial resolution, and non-invasive imaging ability.[7] Several fluorescent probes have been reported to detect ROS variations in the ER, such as $O_2^{\bullet-}$,[8] H_2O_2,[9] and $^1O_2$.[10] These excellent works uncovered the ROS variation in certain ER processes. For instance, $O_2^{\bullet-}$ was found to be generated in the ER during cisplatin-induced cell apoptosis.[8] ClO^- is one of the highly reactive oxygen species (hROS), and is mainly formed from hydrogen peroxide and chloride ions in a myeloperoxidase (MPO)-catalyzed process in living organisms.[11a] The physiological concentration of ClO^- could reach up to 200 μM.[11b] ClO^- is involved in the maintenance of intracellular redox balance, and an abnormal intracellular ClO^- level is tightly relevant to many diseases, such as rheumatoid arthritis and cancers.[12] To this end, numerous fluorescent probes for intracellular ClO^- have been presented, including organelle-localized ClO^-.[13] However, these probes for organelle-localized ClO^- were mainly focused on detection of mitochondrial ClO^-, and the reports on ER-targeted ClO^- imaging are still quite limited, mainly owing to the shortage of dependable detection tools.[14] Additionally, the association between ClO^- variation and ER functions remains far from being understood, indicating the significance of devising new fluorescent probes for monitoring ClO^- variation in the ER region.

In the last few years, we have developed a series of fluorescent probes for mitochondrial ClO^- based on the oxidative hydrolysis of dibenzoylhydrazine.[15] The dibenzoylhydrazine moiety displayed rapid and sensitive response towards ClO^-, while $ONOO^-$, another hROS, might also react with this unit to produce unwanted signal interference.[15c] Therefore, more selective response sites should be considered when we set out to devise an ER-targeted fluorescent probe for ClO^- detection. In 2011, utilizing a ClO^--triggered C=N cleavage reaction, the Lin group developed a probe for ClO^- using a diaminomaleonitrile-derived Schiff base as a reaction site,[16] and this was also applied in the design

[a] *Hubei Collaboration Innovation Center for Biomass Conversion and Utilization, School of Chemistry and Materials Science, Hubei Engineering University, Xiaogan 432000, P. R. China. E-mail: smallcoral@live.cn*
[b] *College of Chemistry and Chemical Engineering, Xinyang Normal University, Xinyang 464000, P. R. China*
[c] *Department of Chemistry, Korea University, Seoul 02841, Korea. E-mail: jongskim@korea.ac.kr*
[d] *School of Chemistry and Chemical Engineering, Tianjin University of Technology, Tianjin, 300384, P. R. China. E-mail: zlt1981@126.com*
[e] *Department of Radiology, The Affiliated Hospital of Southwest Medical University, Luzhou 646000, P. R. China. E-mail: xrenwenxiux@hotmail.com*
[f] *Nuclear Medicine and Molecular Imaging Key Laboratory of Sichuan Province, Luzhou, 646000, P. R. China*

† Electronic supplementary information (ESI) available: Synthesis methods and supplementary figures. See DOI: 10.1039/c9cc00066f

‡ These authors contributed equally to this work.

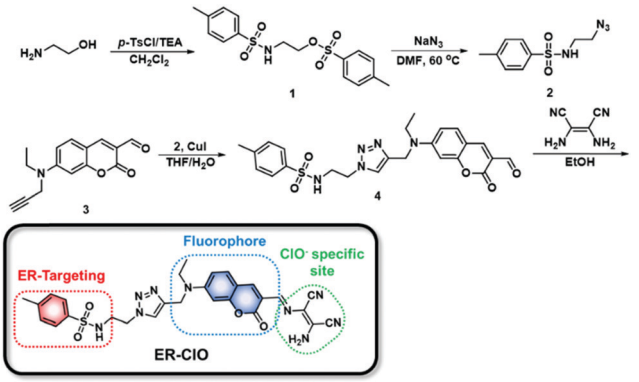

Scheme 1 The synthetic scheme and structure of **ER-ClO**.

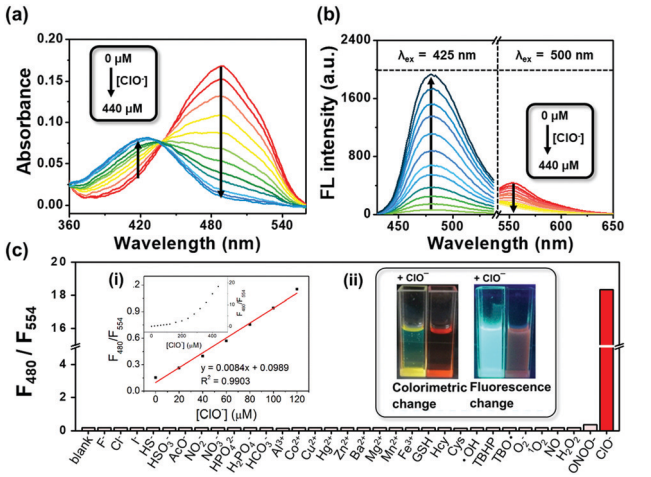

Fig. 1 (a) UV-vis absorption and (b) fluorescence spectra changes of **ER-ClO** (10 μM) in DMF/PBS solution (v/v = 5/5, pH 7.4, 10 mM) upon addition of an increasing amount of ClO^- (0–440 μM). Each spectrum was recorded after **ER-ClO** was incubated with ClO^- for 1 min. For λ_{em} = 554 nm, λ_{ex} = 425 nm, slits: 2.5/2.5 nm; for λ_{em} = 588 nm, λ_{ex} = 500 nm, slits: 5/5 nm. (c) Fluorescence emission intensity ratios (F_{480}/F_{554}) of **ER-ClO** (10 μM) in DMF/PBS solution (v/v = 1/1, pH 7.4, 10 mM) in the presence of various small molecule species (0.5 mM) and ROS/RNS (0.5 mM). Inset: (i) Linear relationship between the fluorescence intensity ratio (F_{480}/F_{554}) of **ER-ClO** (10 μM) *versus* concentration of ClO^-. (ii) The colorimetric and fluorescent changes of the probe in the presence of ClO^-.

of ClO^- specific probes by other research groups.[12a,17] The diaminomaleonitrile-derived Schiff base exhibited excellent selectivity and sensitivity toward ClO^- without interference from other ROS including $ONOO^-$, and was facilely introduced to the fluorophores. On the other hand, the methyl sulfonamide group has been demonstrated to be able to deliver cargo to the ER.[9a,18] Taken together, we introduced a methyl sulfonamide group and diaminomaleonitrile into the 7-diethylamino-coumarin platform, to construct an ER-targeted fluorescent probe **ER-ClO** for ClO^- sensing. The probe was synthesized *via* a simple procedure (Scheme 1) and characterized by ^{1}H NMR, ^{13}C NMR and HRMS (ESI†).

Initially, we tested the optical response of **ER-ClO** to ClO^-. In DMF–phosphate buffer saline (PBS) (v/v = 5/5, pH 7.4, 10 mM) media, **ER-ClO** displayed a main absorption band at 488 nm (Fig. 1a). Upon the addition of ClO^- (0–440 μM), the absorption band at 488 nm gradually decreased, and a new band around 425 nm appeared with an isosbestic point at 437 nm. The absorbance ratio (A_{425}/A_{488}) of **ER-ClO** linearly increased *versus* concentration of ClO^- in the range of 0–120 μM (Fig. S1a, ESI†). Concomitantly, the reaction with ClO^- prompted the emission wavelength of **ER-ClO** to blue-shift from 554 to 480 nm (Fig. 1b). The emission intensity ratio (F_{480}/F_{554}) also exhibited a linear enhancement when the concentration of ClO^- increased from 0 μM to 120 μM (Fig. S1b, ESI†). The detection limit (S/N = 3) of **ER-ClO** toward ClO^- was calculated to be 0.59 μM, which is comparable to those reported previously.[13–15]

After the demonstration of the optical response to ClO^-, the selectivity of **ER-ClO** toward ClO^- was checked. To the solution of 10 μM **ER-ClO**, various common anions (F^-, HS^-, HSO_3^-, Cl^-, HPO_4^{2-}, AcO^-, NO_2^-, NO_3^-, I^-, $H_2PO_4^-$, HCO_3^-), cations (Al^{3+}, Co^{2+}, Cu^{2+}, Hg^{2+}, Zn^{2+}, Ba^{2+}, Mg^{2+}, Mn^{2+}, Fe^{3+}), biothiols (GSH, Hcy, Cys), ROS ($^{\bullet}OH$, *tert*-butyl hydroperoxide (TBHP), *tert*-butoxyl radical ($TBO^{\bullet}$), $O_2^{\bullet-}$, $^1O_2$, $ONOO^-$, H_2O_2, and ClO^-), and NO was added respectively. As depicted in Fig. S2 (ESI†), no significant changes were observed in the absorption spectra when other tested species were added except Hg^{2+} and $ONOO^-$, which could induce a moderate decrement in the absorption band at 488 nm. On the other hand, the original absorbance at 488 nm thoroughly disappeared upon the addition of ClO^- and a new band at 425 nm was found, accompanied by a visible color change from red to yellow (inset in Fig. 1c). Similar responses were observed in the fluorescence spectra. The quenching of the emission at 554 nm and the generation of a new emission peak at 480 nm could only be found in the presence of ClO^- with the fluorescence color changing from orange red to cyan (Fig. 1c and Fig. S3, ESI†). The emission intensity ratio (F_{480}/F_{554}) of **ER-ClO** was increased from 0.18 to 18.35 in the presence of 10 eq. ClO^-, nearly 100-fold ratio enhancement. The above results suggested that **ER-ClO** displayed excellent sensitivity and selectivity toward ClO^- among all the tested small molecule species with dual modes in a ratiometric manner, indicating its potential in the quantitative analysis of ClO^-.

Subsequently, the time-dependent fluorescence ratio changes of **ER-ClO** with ClO^- were explored (Fig. S4a, ESI†). The emission intensity ratio (F_{480}/F_{554}) of **ER-ClO** initially kept steady, while a sharp increment was obtained and saturated in about 30 s when excess ClO^- was added. These results indicated good stability and rapid response capability of the probe. Furthermore, the fluorescence response of **ER-ClO** to ClO^- under different pH was investigated (Fig. S4b, ESI†). In the absence of ClO^-, the probe showed no significant fluorescence ratio changes in a wide pH range of 4.5–10. In the presence of ClO^-, obvious ratio enhancement was evoked in the pH range of 6–10. Considering the nearly neutral environment in the ER,[19] **ER-ClO** should be suitable for ClO^- imaging in the ER.

To validate the reaction mechanism between **ER-ClO** and ClO^-, the mass analysis was performed. As seen in Fig. S5 (ESI†), after reaction with ClO^-, a strong peak at *m*/*z* 534.1211 was found in the mass spectrum, which corresponded to the carboxylic product **5** ([**5** + Na]$^+$: 534.1418). In the previous reports,[12a,16,17]

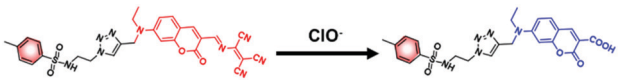

Scheme 2 Proposed reaction mechanism of between **ER-ClO** and ClO^-.

diaminomaleonitrile-derived Schiff base reacted with ClO^- to form the corresponding aldehyde, thus resulting in the fluorescence changes. However, in this case, **ER-ClO** was not converted to coumarin aldehyde by ClO^-, probably owing to the different reactivities of diaminomaleonitrile-derived Schiff bases attached to different fluorophores. Accordingly, the reaction mechanism between **ER-ClO** and ClO^- was proposed in Scheme 2.

The desirable fluorescence properties of **ER-ClO** for ClO^- prompted us to exploit its utility for intracellular ClO^- detection. The cytotoxicity of the probe was first examined. As shown in Fig. S6 (ESI†), more than 80% of the cells stay alive even after incubation with 20 μM **ER-ClO** for 24 h, indicating outstanding biocompatibility of the probe. Then, confocal fluorescent imaging tests were carried out on HeLa cells.

Cultured with 10 μM **ER-ClO** for 30 min at 37 °C in PBS, an apparent fluorescence originating from the probe was observed in the red channel, while it was dim in the blue channel, suggesting the good cell membrane penetrability of the probe (Fig. 2). Upon the addition of exogenous ClO^-, the red fluorescence faded, and the blue emission gradually generated. The ratio of blue fluorescence and red fluorescence rose with an increasing amount of ClO^-, signifying that **ER-ClO** could image intracellular ClO^- in a ratiometric manner.

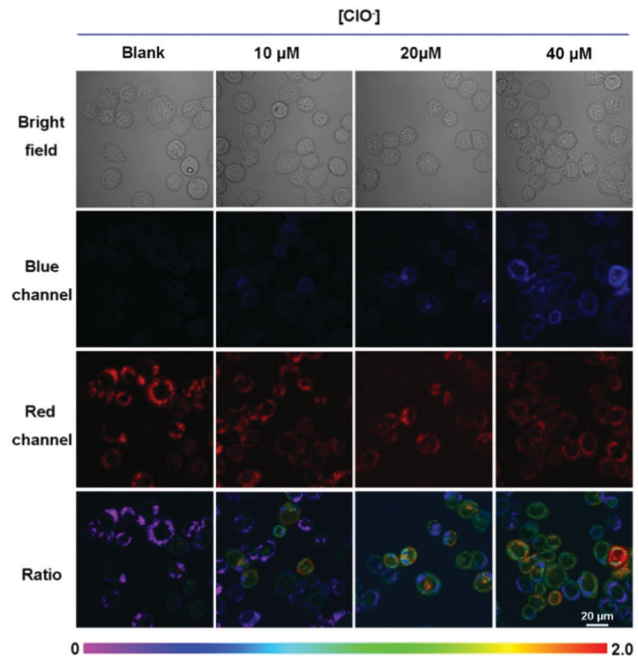

Fig. 2 Confocal fluorescence images of **ER-ClO** in HeLa cells incubated with different concentrations of ClO^-. HeLa cells were incubated with **ER-ClO** (10 μM) at 37 °C for 30 min, and then further treated with different amounts of ClO^- for 30 min. Fluorescence images of HeLa cells from the blue channel (λ_{ex} = 403 nm, λ_{em} = 425–475 nm) and red channel (λ_{ex} = 488 nm, λ_{em} = 552–637 nm). The ratiometric images (F_{blue}/F_{red}) were obtained by mediating the yellow channel image with the related red channel image. Scale bar: 20 μm.

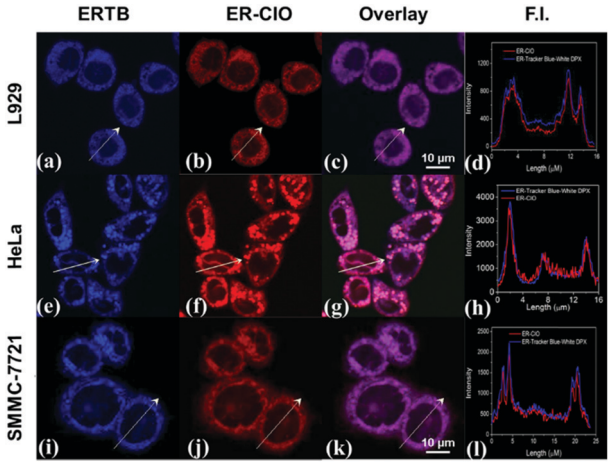

Fig. 3 Confocal fluorescence images of three cell lines stained with (a, e and i) 0.5 μM ERTB (blue channel: λ_{ex} = 403 nm, λ_{em} = 425–475 nm) and (b, f and j) 10 μM **ER-ClO** (red channel: λ_{ex} = 488 nm, λ_{em} = 552–637 nm) at 37 °C for 30 min. (c, g and k) Overlay images. (d, h and l) Intensity profiles of regions of interest (ROI) across cells. Scale bar: 10 μm.

Thereafter, **ER-ClO** was co-cultured with commercial ER trackers to identify its organelle localization in three cell lines (L929, HeLa and SMMC-7721). As illustrated in Fig. 3, the fluorescence of **ER-ClO** was well matched with that of ER-Tracker Blue-White DPX (ERTB) with Pearson's coefficients of 0.93, 0.96, and 0.95 in the three cell lines, respectively, strongly confirming the primary accumulation of the probe in the ER with certain cellular universality. Moreover, the blue fluorescence of the probe generated after the reaction with ClO^- was also demonstrated to root in the ER (Fig. S7, ESI†) using ER-Tracker Red (ERTR) as a control. Additionally, the co-staining experiments of the probe with other commercial organelle dyes, *i.e.* LysoBrite Blue 22642 (LB) for lysosomes and MitoLite Blue FX490 (MB), were performed in L929 cells. As illustrated in Fig. S8 (ESI†), the fluorescence of **ER-ClO** was partially overlapped with that of LTB and MTB with Pearson's coefficients as 0.54 and 0.49, respectively. Combined together, **ER-ClO** possessed prominent ER targetability, which was the cornerstone for detecting the ClO^- in the ER.

Ultimately, **ER-ClO** was utilized to sense endogenous ClO^- in HeLa cells. HeLa cells were pretreated with phorbol 12-myristate 13-acetate (PMA, a ROS stimulant) for 30 min, and then treated with **ER-ClO** for another 30 min. As seen in Fig. 4, compared with the cells treated with the probe only, moderate fluorescence appeared from the blue channel in PMA-stimulated cells with a remarkable ratio change. This result indicated that **ER-ClO** was successfully applied in monitoring the fluctuation of endogenous ClO^- in the ER.

In short, we presented a colorimetric and fluorescent probe **ER-ClO** for the detection of ER ClO^- in a ratiometric manner. This probe rapidly responded to ClO^- with good sensitivity and excellent selectivity. By virtue of the methyl sulfonamide group, the probe was able to accumulate in the ER and was

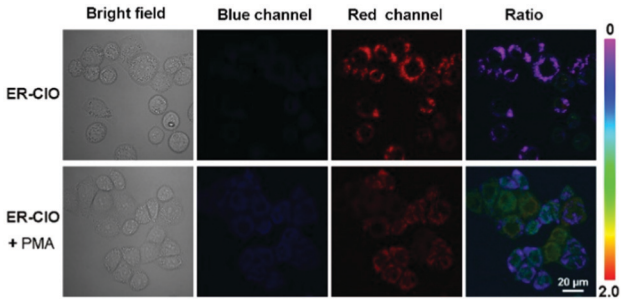

Fig. 4 Confocal fluorescence images of endogenous ClO^- by **ER-ClO**. HeLa cells were incubated with or without PMA at 37 °C for 30 min, and then further treated with **ER-ClO** (10 μM) for another 30 min. For the blue channel: λ_{ex} = 403 nm, λ_{em} = 425–475 nm; for the red channel: λ_{ex} = 488 nm, λ_{em} = 552–637 nm. The ratiometric images (F_{blue}/F_{red}) were obtained by merging the yellow channel image with the related red channel image. Scale bar: 20 μm.

successfully applied in the fluorescence imaging of the exogenous and endogenous ClO^- in the ER. Owing to its desirable properties, **ER-ClO** could be used as an efficient tool in the bioanalysis of disease-associated ClO^- variation in the ER, which could be useful in various biological and clinical applications, and further research is ongoing.

J.-T. H. acknowledges grants from the Hubei Provincial Natural Science Foundation (2018CFB264) and the National Natural Science Foundation of China (no. 21807029); S. W. acknowledges grants from the Hubei Provincial Department of Education Science and Technology Research Projects (No. Q20182704); L. Z. acknowledges grants from the National Natural Science Foundation of China (no. 21203138) and the Natural Science Foundation of Tianjin (No. 17JCYBJC19600); J. S. K. acknowledges grants from CRI project (No. 2018R1A3B1052702).

Conflicts of interest

There are no conflicts to declare.

Notes and references

1 C. Hetz, *Nat. Rev. Mol. Cell Biol.*, 2012, **13**, 89–102.
2 D. E. Clapham, *Cell*, 2007, **131**, 1047–1058.
3 N. Sovolyova, S. Healy, A. Samali and S. E. Logue, *Biol. Chem.*, 2014, **395**, 1–13.
4 (*a*) J. J. M. Hoozemans and W. Scheper, *Int. J. Biochem. Cell Biol.*, 2012, **44**, 1295–1298; (*b*) J. Jeong, J. M. Walker, F. Wang, J. G. Park, A. E. Palmer, C. Giunta, M. Rohrbach, B. Steinmann and D. J. Eide, *Proc. Natl. Acad. Sci. U. S. A.*, 2012, **109**, E3530; (*c*) R. J. Deshaies, *BMC Biol.*, 2014, **12**, 94; (*d*) G. C. Shore, F. R. Papa and S. A. Oakes, *Curr. Opin. Cell Biol.*, 2011, **23**, 143–149; (*e*) I. Kim, W. Xu and J. C. Reed, *Nat. Rev. Drug Discovery*, 2008, **7**, 1013–1030; (*f*) J. H. Lin, P. Walter and T. S. Yen, *Annu. Rev. Pathol.: Mech. Dis.*, 2008, **3**, 399–425.
5 (*a*) J. S. Nam, M. G. Kang, J. Kang, S. Y. Park, S. J. C. Lee, H. T. Kim, J. K. Seo, O. H. Kwon, M. H. Lim, H. W. Rhee and T. H. Kwon, *J. Am. Chem. Soc.*, 2016, **138**, 10968–10977; (*b*) Z. Feng, H. Wang, S. Wang, Q. Zhang, X. Zhang, A. A. Rodal and B. Xu, *J. Am. Chem. Soc.*, 2018, **140**, 9566–9573.
6 (*a*) L. Tong, R. A. Heim and S. Wu, *Free Radical Biol. Med.*, 2011, **50**, 1717–1725; (*b*) T. Uehara, T. Nakamura, D. Yao, Z.-Q. Shi, Z. Gu, Y. Ma, E. Masliah, Y. Nomura and S. A. Lipton, *Nature*, 2006, **441**, 513–517.
7 (*a*) J.-T. Hou, W. X. Ren, K. Li, J. Seo, A. Sharma, X.-Q. Yu and J. S. Kim, *Chem. Soc. Rev.*, 2017, **46**, 2076–2090; (*b*) M. Li, H. Ge, V. Mirabello, R. L. Arrowsmith, G. Kociok-Kohn, S. W. Botchway, W. Zhu, S. I. Pascu and T. D. James, *Chem. Commun.*, 2017, **53**, 11161–11164; (*c*) K. Gu, Y. Xu, H. Li, Z. Guo, S. Zhu, S. Zhu, P. Shi, T. D. James, H. Tian and W.-H. Zhu, *J. Am. Chem. Soc.*, 2016, **138**, 5334–5340; (*d*) S. Kolemen and E. U. Akkaya, *Coord. Chem. Rev.*, 2018, **354**, 121–134; (*e*) M. L. Odyniec, A. C. Sedgwick, A. H. Swan, M. Weber, T. M. S. Tang, J. E. Gardiner, M. Zhang, Y.-B. Jiang, G. Kociok-Kohn, R. B. P. Elmes, S. D. Bull, X.-P. He and T. D. James, *Chem. Commun.*, 2018, **54**, 8466–8469; (*f*) A. C. Sedgwick, H.-H. Han, J. E. Gardiner, S. D. Bull, X.-P. He and T. D. James, *Chem. Sci.*, 2018, **9**, 3672–3676; (*g*) A. C. Sedgwick, L. Wu, H.-H. Han, S. D. Bull, X.-P. He, T. D. James, J. L. Sessler, B. Z. Tang, H. Tian and J. Yoon, *Chem. Soc. Rev.*, 2018, **47**, 8842–8880; (*h*) A. C. Sedgwick, W.-T. Dou, J.-B. Jiao, L. Wu, G. T. Williams, A. T. A. Jenkins, S. D. Bull, J. L. Sessler, X.-P. He and T. D. James, *J. Am. Chem. Soc.*, 2018, **140**, 14267–14271.
8 H. Xiao, X. Liu, C. Wu, Y. Wu, P. Li, X. Guo and B. Tang, *Biosens. Bioelectron.*, 2017, **91**, 449–455.
9 (*a*) H. Xiao, P. Li, X. Hu, X. Shi, W. Zhang and B. Tang, *Chem. Sci.*, 2016, **7**, 6153–6159; (*b*) C. Gao, Y. Tian, R. Zhang, J. Jing and X. Zhang, *Anal. Chem.*, 2017, **89**, 12945–12950.
10 H. Bian, X. Song, N. Li, H. Man and Y. Xiao, *J. Mater. Chem. B*, 2018, **6**, 1699–1705.
11 (*a*) Y. W. Yap, M. Whiteman and N. S. Cheung, *Cell. Signalling*, 2007, **19**, 219–228; (*b*) T. G. Favero, D. Colter, P. F. Hooper and J. J. Abramson, *J. Appl. Physiol.*, 1998, **84**, 425–430.
12 (*a*) H. Feng, Z. Zhang, Q. Meng, H. Jia, Y. Wang and R. Zhang, *Adv. Sci.*, 2018, **5**, 1800397; (*b*) C. Gorrini, I. S. Harris and T. W. Mak, *Nat. Rev. Drug Discovery*, 2013, **12**, 931–947.
13 (*a*) B. Zhang, X. Yang, R. Zhang, Y. Liu, X. Ren, M. Xian, Y. Ye and Y. Zhao, *Anal. Chem.*, 2017, **89**, 10384–10390; (*b*) X. Chen, F. Wang, J. Y. Hyun, T. Wei, J. Qiang, X. Ren, I. Shin and J. Yoon, *Chem. Soc. Rev.*, 2016, **45**, 2976–3016; (*c*) H. Zhu, J. Fan, J. Wang, H. Mu and X. Peng, *J. Am. Chem. Soc.*, 2014, **136**, 12820–12823; (*d*) Y. Huang, P. Zhang, M. Gao, F. Zeng, A. Qin, S. Wu and B. Z. Tang, *Chem. Commun.*, 2016, **52**, 7288–7291; (*e*) Y. L. Pak, S. J. Park, D. Wu, B. Cheon, H. M. Kim, J. Bouffard and J. Yoon, *Angew. Chem., Int. Ed.*, 2018, **57**, 1567–1571; (*f*) J. J. Hu, N.-K. Wong, M.-Y. Lu, X. Chen, S. Ye, A. Q. Zhao, P. Gao, R. Y.-T. Kao, J. Shen and D. Yang, *Chem. Sci.*, 2016, **7**, 2094–2099; (*g*) L. Yuan, L. Wang, B. K. Agrawalla, S.-J. Park, H. Zhu, B. Sivaraman, J. Peng, Q.-H. Xu and Y.-T. Chang, *J. Am. Chem. Soc.*, 2015, **137**, 5930–5938; (*h*) B. Zhu, L. Wu, M. Zhang, Y. Wang, C. Liu, Z. Wang, Q. Duan and P. Jia, *Biosens. Bioelectron.*, 2018, **107**, 218–223.
14 (*a*) J.-P. Li, S. Xia, H. Zhang, G.-R. Qu and H.-M. Guo, *Sens. Actuators, B*, 2018, **255**, 622–629; (*b*) Y. L. Pak, S. J. Park, G. Song, Y. Yim, H. Kang, H. M. Kim, J. Bouffard and J. Yoon, *Anal. Chem.*, 2018, **90**, 12937–12943.
15 (*a*) J.-T. Hou, M.-Y. Wu, K. Li, J. Yang, K.-K. Yu, Y.-M. Xie and X.-Q. Yu, *Chem. Commun.*, 2014, **50**, 8640–8643; (*b*) J.-T. Hou, K. Li, J. Yang, K.-K. Yu, Y.-X. Liao, Y.-Z. Ran, Y.-H. Liu, X.-D. Zhou and X.-Q. Yu, *Chem. Commun.*, 2015, **51**, 6781–6784; (*c*) K. Li, J.-T. Hou, J. Yang and X.-Q. Yu, *Chem. Commun.*, 2017, **53**, 5539–5541.
16 L. Yuan, W. Lin, J. Song and Y. Yang, *Chem. Commun.*, 2011, **47**, 12691–12693.
17 G. Li, Q. Lin, L. Sun, C. Feng, P. Zhang, B. Yu, Y. Chen, Y. Wen, H. Wang, L. Ji and H. Chao, *Biomaterials*, 2015, **53**, 285–295.
18 S. Xu, H.-W. Liu, X.-X. Hu, S.-Y. Huan, J. Zhang, Y.-C. Liu, L. Yuan, F.-L. Qu, X.-B. Zhang and W. Tan, *Anal. Chem.*, 2017, **89**, 7641–7648.
19 J. R. Casey, S. Grinstein and J. Orlowski, *Nat. Rev. Mol. Cell Biol.*, 2010, **11**, 50–61.

